Adaptive control of hypersonic vehicles in the presence of modeling uncertainties

Citation: Gibson, T.E., L.G. Crespo, and A.M. Annaswamy. "Adaptive control of hypersonic vehicles in the presence of modeling uncertainties." American Control Conference, 2009. ACC '09. 2009. 3178-3183. ©2009 Institute of Electrical and Electronics Engineers.

As Published: http://dx.doi.org/10.1109/ACC.2009.5160746

Publisher: Institute of Electrical and Electronics Engineers

Persistent URL: http://hdl.handle.net/1721.1/59334

Version: Final published version: final published article, as it appeared in a journal, conference proceedings, or other formally published context

2009 American Control Conference
Hyatt Regency Riverfront, St. Louis, MO, USA
June 10-12, 2009

Adaptive Control of Hypersonic Vehicles in the Presence of Modeling Uncertainties

Travis E. Gibson, Luis G. Crespo, and Anuradha M. Annaswamy

***Abstract*— This paper proposes an adaptive controller for a hypersonic cruise vehicle subject to aerodynamic uncertainties, center-of-gravity movements, actuator saturation, failures, and time-delays. The adaptive control architecture is based on a linearized model of the underlying rigid body dynamics and explicitly accommodates for all uncertainties. It also includes a baseline proportional integral filter commonly used in optimal control designs. The control design is validated using a high-fidelity HSV model that incorporates various effects including coupling between structural modes and aerodynamics, and thrust pitch coupling. An elaborate comparative analysis of the proposed Adaptive Robust Controller for Hypersonic Vehicles (ARCH) is carried out using a control verification methodology. In particular, we study the resilience of the controller to the uncertainties mentioned above for a set of closed-loop requirements that prevent excessive structural loading, poor tracking performance and engine stalls. This analysis enables the quantification of the improvements that result from using and adaptive controller for a typical maneuver in the $V-h$ space under cruise conditions.**

I. Introduction

Over the past decade a significant amount of work has been performed on *Hypersonic Vehicle* (HSV) modeling. These models are of varying levels of fidelity and incorporate some or all of the following: thrust-pitch coupling [1], elastic-rigid body coupling [2], [3], and viscous and unsteady effects [4]. More recently, non-adaptive and adaptive control designs have been proposed for the control of hypersonic vehicles, in [5], [6], [7], [8] and [9], [10], [11], [12], [13], respectively. The uncertainties that have been considered include geometric and inertial [6], [12], aerodynamic [7], [11], and inertial-elastic [8]. In [10], [7] and [8], the control inputs used include the canard which increases the available bandwidth for the controller. In [8], [11] and [13] the canard is not used as a control input.

In this paper, we propose an adaptive controller using only the equivalence ratio and the elevator deflection as control inputs. Uncertainties in the pitching moment, lift force, mass, and Center-of-Gravity position are introduced. Actuators are subjected to magnitude saturation. The adaptive controller is designed by neglecting the flexible effects and their coupling with the vehicle dynamics, but is evaluated with the latter as well as time-delays present. The stability and robustness of the underlying adaptive system has been studied elsewhere.[14][15]

This work was supported by NASA Grant No. NNX07AC48A

T. E. Gibson (tgibson@mit.edu) and A. M. Annaswamy are both with the Department of Mechanical Engineering, Massachusetts Institute of Technology, Cambridge MA, 02139, USA

L. G. Crespo is with the National Institute of Aerospace, Hampton VA, 23666, USA

The control verification methodology proposed in [16] is used herein to quantify the improvements in robust performance that result from augmenting the baseline controller with an adaptive component. The rationale behind this analysis is the determination of the largest hyper-rectangular set in the uncertain parameter space for which the closed-loop specifications are satisfied. This framework ignores the assumptions made during control design to provide a control assessment that only depends on the performance and robustness observed during simulation.

II. Hypersonic Vehicle Modeling

Two hypersonic vehicle models will be used throughout this paper, one as a *Design Model* (DM) to carry out the control design, and one as an *Evaluation Model* (EM) to validate the proposed design by including more effects that are typically present in real aircraft. Both models pertain to the longitudinal dynamics of a hypersonic vehicle. The DM includes the rigid body dynamics of the vehicle, with the following five states: height h, velocity V, angle of attack α, euler angle θ, and pitch rate, q. The governing equations for the DM are shown below,

$$\begin{aligned} \dot{V} &= (\mathcal{T}\cos\alpha - D)/m - g\sin\gamma \\ \dot{\alpha} &= (-\mathcal{T}\sin\alpha - L)/mV + q + g\cos(\gamma/V) \\ \dot{q} &= M/I_{yy} \quad \dot{h} = V\sin\gamma \quad \dot{\theta} = q, \end{aligned} \tag{1}$$

where $\mathcal{T}$, D, M, m, I_{yy}, g and γ are the thrust, drag, pitching moment, mass, moment of inertia, gravitational constant and flight path angle respectively. The flight path angle is defined as $\gamma = \theta - \alpha$.

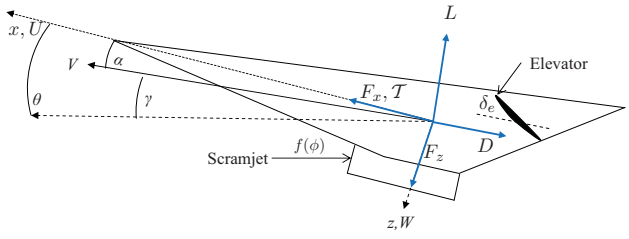

Fig. 1. Axes of the HSV

The control inputs for the model are the equivalence ratio into the scramjet combustor, ϕ, and the elevator deflection angle, δ_e. The control inputs indirectly affect the dynamics of the aircraft by appearing in the forcing terms, $\mathcal{T}$, D, and M. A side view of the HSV with the control inputs and axes can be seen in Figure 1.

The evaluation model encompasses rigid-elastic state coupling, and is described by the following:

$$\begin{aligned}
\dot{V} &= (\mathcal{T}\cos\alpha - D)/m - g\sin\gamma \\
\dot{\alpha} &= -(\mathcal{T}\sin\alpha + L)/mV + q + g\cos(\gamma/V) \\
\dot{q} &= (M + \tilde{\psi}_f\ddot{\eta}_f + \tilde{\psi}_a\ddot{\eta}_a)/I_{yy} \\
\dot{h} &= V\sin\gamma \quad \dot{\theta} = q \\
k_f\ddot{\eta}_f &= -2\zeta_f\omega_f\dot{\eta}_f - \omega_f^2\eta_f + N_f - \frac{\tilde{\psi}_f M}{I_{yy}} - \frac{\tilde{\psi}_f\tilde{\psi}_a\ddot{\eta}_f}{I_{yy}} \\
k_a\ddot{\eta}_a &= -2\zeta_a\omega_a\dot{\eta}_a - \omega_a^2\eta_a + N_a - \frac{\tilde{\psi}_a M}{I_{yy}} - \frac{\tilde{\psi}_f\tilde{\psi}_a\ddot{\eta}_a}{I_{yy}},
\end{aligned} \tag{2}$$

where η_a and η_f are the elastic states, N_a and N_f are the elastic forcing terms, ζ_a and ζ_f the damping terms, ω_a and ω_f the natural frequencies and $\tilde{\psi}_a$, $\tilde{\psi}_f$, k_a, and k_f are the modal weighting terms. The subscripts f and a in the elastic terms denote forward and aft respectively. For more details pertaining to the elastic terms refer to [7], with support from Reference [2].

Actuator dynamics will also be incorporated into the design and evaluation models. These can be described as follows:

$$\begin{aligned}
\ddot{\phi} &= -2\zeta_\phi\omega_\phi\dot{\phi} - \omega_\phi^2\phi + \omega_\phi\phi_{\text{cmd}} \\
\ddot{\delta}_e &= -2\zeta_\delta\omega_\delta\dot{\delta}_e - \omega_\delta^2\delta_e + \omega_\delta\delta_{e,\text{cmd}}
\end{aligned} \tag{3}$$

with $\zeta_\phi = 1,\ \zeta_{\delta_e} = 1,\ \omega_\phi = 10$ and $\omega_\delta = 20$.

The control design methodology proposed in the paper is based on a linearized model of the DM. The EM is subsequently used to validate the control design. It should be noted that the linearized model of the DM and the EM coincide when the elastic effects are neglected. However, both the DM and EM are included above for ease of exposition.

III. Linearized Model

The underlying design model, described by the DM in (1) and the actuator dynamics in (3) can be expressed compactly as a nonlinear model

$$\dot{X} = f(X, U), \tag{4}$$

where X is the state vector and U contains the exogenous inputs ϕ_{cmd} and $\delta_{e,\text{cmd}}$. In order to facilitate the control design, we linearize these equations at the trim state X_0 and trim input U_0 satisfying $f(X_0, U_0) = 0$ in order to obtain the following:

$$\dot{x}_p = A_p x_p + B_p u + \varepsilon(t), \tag{5}$$

where ε is the linearization error, which is assumed to be small,

$$\begin{aligned}
A_p &= \left.\frac{\partial f(X,U)}{\partial X}\right|_{\substack{X=X_0\\U=U_0}},\quad B_p = \left.\frac{\partial f(X,U)}{\partial U}\right|_{\substack{X=X_0\\U=U_0}}, \\
x_p &= X - X_0,\ \text{ and }\ u = U - U_0.
\end{aligned} \tag{6}$$

The linear state x_p contains the perturbation states, $[\Delta V\ \ \Delta\alpha\ \ \Delta q\ \ \Delta h\ \ \Delta\theta\ \ \Delta\dot{\phi}\ \ \Delta\phi\ \ \Delta\dot{\delta}_e\ \ \Delta\delta_e]^T$ and u is the command input perturbation vector, $[\Delta\phi_{\text{cmd}}\ \Delta\delta_{e,\text{cmd}}]^T$.

Integral error states will be augmented to the linear model of the HSV. The reference command , r, will be given in $h - V$ space and is constructed as

$$r = [\Delta V_{\text{ref}}\ \ \Delta h_{\text{ref}}]^T \tag{7}$$

Denoting an output $y = [\Delta V\ \ \Delta h]^T$ an integral error state e_I is constructed as

$$e_I = \int(y - r)d\tau = \int(Hx_p - r)d\tau, \tag{8}$$

where H is a selection matrix. In addition to error augmentation, the actuator inputs will be explicitly incorporated into the linear model as states, and a new input v is introduced as

$$v = \dot{u}. \tag{9}$$

By augmenting both the command following error in (8) and actuator inputs in (9) to the linear system in (5), the overall linear system becomes,

$$\underbrace{\begin{bmatrix}\dot{x}_p\\ \dot{e}_I\\ \dot{u}\end{bmatrix}}_{\dot{x}} = \underbrace{\begin{bmatrix}A_p & 0 & B_p\\ H & 0 & 0\\ 0 & 0 & 0\end{bmatrix}}_{A}\underbrace{\begin{bmatrix}x_p\\ e_I\\ u\end{bmatrix}}_{x} + \underbrace{\begin{bmatrix}0\\0\\I\end{bmatrix}}_{B} v + \underbrace{\begin{bmatrix}0\\-I\\0\end{bmatrix}}_{B_{\text{cmd}}} r, \tag{10}$$

which can be compactly expressed as,

$$\dot{x} = Ax + Bv + B_{\text{cmd}}r. \tag{11}$$

IV. Control Design and Uncertainty

The control structure proposed in this paper has a combination of feedforward input, nominal feedback, and adaptive feedback terms. Two parameter vectors p and d are introduced, where p denotes a vector of uncertain parameters while d denotes a vector of free design parameters in the baseline and adaptive controllers. The roles of d and p will be covered in more detail in the subsequent section.

A. Baseline Controller

The baseline controller is chosen as an LQ regulator, so that a cost function of the form

$$J = \int(\tilde{x}^T Q_x \tilde{x} + v^T R_v v)d\tau \tag{12}$$

is minimized, where $\tilde{x} = x - x^*$, and x^* is the steady-state value that x will converge to for a constant reference input.[1] The weighting matrices Q_x and R_v are suitably chosen positive definite diagonal matrices.

After minimization of the cost function in (12), the control input is of the form

$$v = v_{\text{baseline}} = K_{ff}r + K^T x \tag{13}$$

Noting that the components of x include the integral e_I, and u, it follows that the baseline controller has *Proportional*, *Integral*, and *Filter* components, thus, leading to a PIF-LQ regulator as first introduced in [18] with more details given in [17]. The PIF control structure is shown in Figure 2.

[1]The construction of $\tilde{x}$ is covered in great detail in Reference [17] page 523 and PIF control structure on pages 528-531.

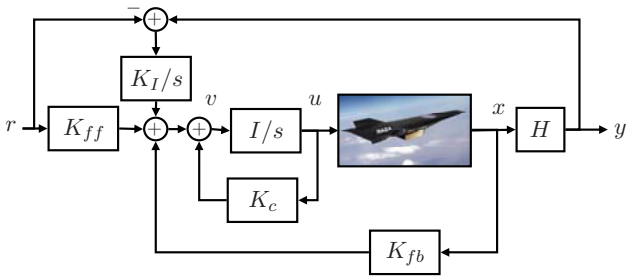

Fig. 2. PIF control structure. [11], [18], [17]

B. Uncertainties and Actuator Saturation

The uncertainties to be considered are lumped into the vector

$$p = [\lambda, \ \tau]^T = [\lambda_m \ \ \lambda_L \ \ \lambda_M \ \ \Lambda_{CG} \ \ \tau]^T, \tag{14}$$

whose components are as follows

1) Multiplicative uncertainty in the inertial properties: $m = \lambda_m m_0$, and $I_{yy} = \lambda_m I_{yy0}$ where $\lambda_m \in (0, 2]$.
2) Multiplicative uncertainty in lift: $C_L^\alpha = \lambda_L C_{L,0}^\alpha$, where $\lambda_L \in (0, 2]$.
3) Multiplicative uncertainty in pitching moment: $C_M^\alpha = \lambda_M C_{M,0}^\alpha$, where $\lambda_M \in (0, 2]$.
4) Longitudinal distance between the neutral point and the center of gravity divided by the mean aerodynamic chord is denoted as $\lambda_{CG} \in [-0.1, 0.1]$. Negative values of λ_{CG} denote that the CG has been moved toward the aft of the HSV.
5) Uncertain time-delay in all plant inputs where $\tau \in (0, 0.04s]$.

The nominal value of the uncertain parameter vector is given by.

$$\bar{p} = [1 \ \ 1 \ \ 1 \ \ 0 \ \ 0]^T. \tag{15}$$

The components of λ are considered parametric uncertainties and the flexible effects and time delay are considered non–parametric uncertainties. While τ is a parameter as well, it is not introduced as a component of λ since the underlying design model is finite–dimensional, and is treated as a non–parametric uncertainty. The state jacobian of the uncertain design model is defined as $A_{p,\text{uncertain}} = A_p(\lambda)$ and in combination with the DM plant dynamics in (5) results in the following uncertain plant dynamics,

$$\dot{x}_p = A_p(\lambda)x_p + B_p u. \tag{16}$$

The adaptive control design that follows will explicitly account for the parametric uncertainty λ while remaining robust with respect to τ and the other non–parametric uncertainties associated with the elastic effects.

In addition to the above uncertainties, our studies also include magnitude saturation in the actuators. This is accounted for with the inclusion of a rectangular saturation function $R_s(u)$ where the i-th component is defined as,

$$R_{s_i} = \begin{cases} u_i & \text{if } u_{\min_i} \le u_i \le u_{\max_i}, \\ u_{\max_i} & \text{if } u_i > u_{\max_i}, \\ u_{\min_i} & \text{if } u_i < u_{\min_i} \end{cases} \tag{17}$$
$$\text{for } i = 1, 2.$$

C. Adaptive Controller

In order to compensate for the modeling uncertainties, an adaptive controller is now added to the baseline controller. The structure of the adaptive controller is chosen as

$$v = \overbrace{K_{ff} r + \underbrace{K^T x}_{\text{nominal}}}^{\text{baseline}} + \underbrace{\theta(t)^T x}_{\text{adaptive}} \tag{18}$$

The adaptive component of the controller is denoted θ and is the same dimension as the nominal feedback gain K. The adaptive component naturally augments the nominal controller and a visual interpretation of this can be seen in Figure 3.

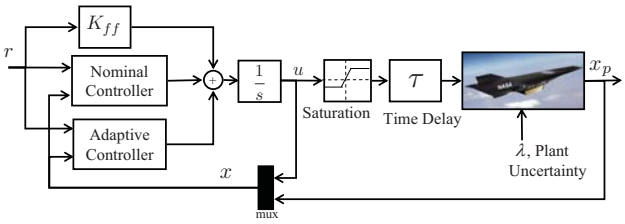

Fig. 3. Baseline with adaptive augmentation and uncertainty

Combining the uncertain plant model in (16) with the integral state e_I in (8), the input-state in (9), the the saturation function in (17), and the overall baseline and adaptive control input from (18), the closed loop equations are given by,

$$\underbrace{\begin{bmatrix} \dot{x}_p \\ \dot{e} \\ \dot{u} \end{bmatrix}}_{\dot{x}} = \underbrace{\begin{bmatrix} A_p(\lambda) & 0 & B_p \\ H & 0 & 0 \\ K_1 + \theta_1(t) & K_2 + \theta_2(t) & K_3 + \theta_3(t) \end{bmatrix}}_{A(\lambda)+B(K^T+\theta(t)^T)} \underbrace{\begin{bmatrix} x_p \\ e \\ u \end{bmatrix}}_{x} + \underbrace{\begin{bmatrix} 0 \\ -I \\ K_{ff} \end{bmatrix}}_{B_m} r - \underbrace{\begin{bmatrix} B_p \\ 0 \\ 0 \end{bmatrix}}_{B_1} u_\Delta, \tag{19}$$

where $u_\Delta = u - R_s(u)$, and in compact form reduces to,

$$\dot{x} = (A(\lambda) + B(K^T + \theta(t)^T))x + B_m r - B_1 u_\Delta. \tag{20}$$

A reference model is chosen as

$$\dot{x}_m = A_m x_m + B_m r. \tag{21}$$

where A_m and B_m are such that A_m is a Hurwitz matrix, $B_m = B_{\text{cmd}} K_{ff}$, $\theta*$ is an ideal value of θ such that $\bar{A}_m = A(\lambda) + B(K^T + \theta^{*T})$ and $A_\Delta = \bar{A}_m - A_m$. We note that due to the addition of the integral action in the filter, it may not

be possible to choose A_Δ to be zero for general parametric uncertainties. Defining the reference model error e as,

$$e = x - x_m, \tag{22}$$

we choose adaptive laws for adjusting the adaptive parameter in (18) as

$$\begin{aligned} \dot{\theta} &= -\Gamma_\theta x e_a^T P B \\ \dot{\hat{A}}_\Delta &= \Gamma_A P e_a x^T \end{aligned} \tag{23}$$

where $A_m^T P + P A_m^T = -Q$ and $Q = Q^T > 0$.[19] Also $e_a = e - e_\Delta$ where the auxiliary error e_Δ is defined as,

$$\dot{e}_\Delta = A_m e_\Delta + \hat{A}_\Delta x - B_1 u_\Delta. \tag{24}$$

The auxiliary error represents the error that occurs do to saturation and reference model mismatch, and subtracting it from e we obtain the augmented error e_a which is the error due to parameter mismatch. In the above adaptive laws Γ_θ, Γ_A and Q are free design parameters.[2]

Theorem 1: For all initial conditions of the state vector x and adaptive gain θ inside a bounded set, the system in (16) with the controller in (18) and the adaptive law in (23) has bounded trajectories for all time.

Remark 1: The proof of stability is an extension of Karason and Annaswamy's work in [21] with some similarities to [14]. With the addition of the filter however, the control input is not implemented through u, but rather through $\dot{u}$. This in turn leads to u becoming a part of the state vector x.

With the complete control design given, all of the free design parameters of the overall controller can be combined into a single vector d such that,

$$d = [q_x \;\; r_v \;\; \gamma_\theta \;\; \gamma_A \;\; q]. \tag{25}$$

where the elements in d are the diagonal elements of Q_x, R_v, Γ_θ, Γ_A and Q respectively. Each simulation result is completely defined by the control design vector d and the uncertain parameter vector p. These two vectors are utilized extensively in the control verification section.

V. Control Verification

In this section we evaluate the improvements resulting from augmenting the baseline controller with an adaptive component. This is attained by determining the largest hyper-rectangular set in the uncertain parameter space p for which a set of closed-loop requirements are satisfied by all the set members. The section that follows presents a brief introduction to the mathematical framework required to perform this study. References [16] and [22] cover this material in detail.

A. Mathematical Framework

The parameters which specify the closed-loop system are grouped into two categories: uncertain parameters, which are denoted by the vector p, and the control design parameters, which are denoted by the vector d. While the plant model depends on p, the controller depends on d. The *Nominal Parameter* value, denoted as $\bar{p}$, is a deterministic estimate of the true value of p.

Stability and performance requirements for the closed-loop system will be prescribed by the set of inequality constraints, $g(p, d) < 0$. Throughout this paper, it is assumed that vector inequalities hold component wise. For a fixed d, the larger the region in p-space where $g < 0$, the more robust the controller.

The *Failure Domain* corresponding to the controller with parameters d is given by[3]

$$\mathcal{F}^j(d) = \{p : g_j(p, d) \geq 0\}, \tag{26}$$

$$\mathcal{F}(d) = \bigcup_{j=1}^{\dim(\boldsymbol{g})} \mathcal{F}^j(d). \tag{27}$$

While Equation (26) describes the failure domain corresponding to the jth requirement, Equation (27) describes the failure domain for all requirements. The *Non-Failure Domain* is the complement set of the failure domain and will be denoted[4] as $C(\mathcal{F})$. The names "failure domain" and "non-failure domain" are used because in the failure domain at least one constraint is violated while, in the non-failure domain, all constraints are satisfied.

Let Ω be a set in p-space, called the *Reference Set*, whose geometric center is the nominal parameter $\bar{p}$. The geometry of Ω will be prescribed according to the relative levels of uncertainty in p. One possible choice for the reference set is the hyper-rectangle

$$\mathcal{R}(\bar{p}, n) = \{p : \bar{p} - n \leq \; p \leq \bar{p} + n\}. \tag{28}$$

where $n > 0$ is the semi-diagonal of the rectangle. In what follows we assume that $g(\bar{p}, d) < 0$. The tasks of interest is to assign a measure of robustness to a controller based on measuring how much the reference set can be deformed before intersecting the failure domain. A homothet of Ω is given by the set $\{\bar{p} + \alpha(p - \bar{p}) : p \in \Omega\}$, where $\bar{p}$ is the center of the rectangle and $\alpha >$, is the *Similitude Ratio*. While expansions of Ω are accomplished when $\alpha > 1$, contractions result when $0 \leq \alpha < 1$.

Intuitively, one imagines that a homothet of the reference set is being deformed until its boundary touches the failure domain. Any point where the deforming set touches the failure domain is a *Critical Parameter Value* (CPV). The CPV, which will be denoted as $\tilde{p}$, might not be unique. The deformed set is called the *Maximal Set* (MS) and will be denoted as $\mathcal{M}$. The *Critical Similitude Ratio*, denoted as $\tilde{\alpha}$, is the similitude ratio of that deformation. While the critical similitude ratio is a non-dimensional number, the *Parametric Safety Margin* (PSM), denoted as ρ and defined later, is its dimensional equivalent. Both the critical similitude ratio and the PSM quantify the size of the MS. Details on how to

[2]The choice of Γ was driven by an optimal selection function defined in [20].

[3]Throughout this section, super-indices are used to denote a particular vector or set while numerical sub-indices refer to vector components, e.g., p_i^j is the ith component of the vector p^j.

[4]The complement set operator will be denoted as $C(\cdot)$.

calculate the CPV $\tilde{p}$ and $\tilde{\alpha}$ are available in [16].

Once the CPV has been found, the MS is uniquely determined by

$$\mathcal{M}(d) = \mathcal{R}(\bar{p}, \tilde{\alpha}n). \tag{29}$$

The size of this set is proportional to the PSM which is defined as

$$\rho = \tilde{\alpha}\|n\|, \tag{30}$$

Because the critical similitude ratio and the PSM measure the size of the MS, their values are proportional to the degree of robustness of the controller associated with d to uncertainty in p. The critical similitude ratio is non-dimensional, but depends on both the shape and the size of the reference set. The PSM has the same units as the uncertain parameters, and depends on the shape, but not the size, of the reference set. If the PSM is zero, the controller's robustness is practically nil since there are infinitely small perturbations of $\bar{p}$ leading to the violation of at least one of the requirements. If the PSM is positive, the requirements are satisfied for parameter points in the vicinity of the the nominal parameter point. The larger the PSM, the larger the hyper-rectangular-shaped vicinity.

B. Hypersonic Vehicle

The reference set Ω for $p = [\lambda_m, \lambda_L, \lambda_P, \lambda_{CG}, \tau]$ to be used is a hyper-rectangle with aspect vector $n = [1, 1, 1, 0.1, 0.04]$ and nominal parameter point $\bar{p} = [1, 1, 1, 0, 0]$. Note that n determines the relative levels of uncertainty among parameters, e.g., there is $0.04/0.1$ more uncertainty in the CG location than in the time delay.

A set of closed-loop requirements is introduced subsequently. Lets define the vector of signals

$$h(p, d, t) = [\dot{V}(p, d, t) - 10g, |\alpha(p, d, t)| - 0.2, \tag{31}$$

$$\|e_{I,1}(p, d, t)\|_2 - \beta\|e_{I,1}(\bar{p}, d_{base}, t_f)\|_2, \tag{32}$$

$$\|e_{I,2}(p, d, t)\|_2 - \beta\|e_{I,2}(\bar{p}, d_{base}, t_f)\|_2], \tag{33}$$

where $e_{I,1}$ is the velocity error, $e_{I,2}$ is the altitude error, $beta > 1$ is a real number, d_{base} refers to the baseline controller, and t_f is a sufficiently large integration time. This vector enables the formulation of the following set of requirements:

1) Structural: the acceleration at the CG must not exceed $10g$s, i.e., $g_1 = \max_t\{h_1\}$.
2) Stability and engine stall: the angle of attack must stay in the $\pm 0.2\ rad$ range, i.e., $g_2 = max_t\{h_2\}$.
3) Tracking performance in velocity: the tracking error must not exceed a prescribed upper bound, i.e., $g_3 = h_3(t = t_f)$.
4) Tracking performance in altitude: the tracking error must not exceed a prescribed upper bound, i.e., $g_4 = h_4(t = t_f)$.

In the studies that follow the HSV was trimmed at 85,000 ft at a speed of Mach 8. Smooth reference commands were given for a change in velocity of 1,0000 ft/s and a change in altitude of 10,000 ft.[5] We evaluate the robustness characteristics of both controllers for several subsets of $[\lambda_m, \lambda_L, \lambda_P, \lambda_{CG}, \tau]$. Parametric studies indicate that the trim-ability condition $\max\{[u_{max} - U_0, U_0 - u_{min}]\} > 0$, where $f(X_0, U_0, p) = 0$ for the saturation limits $u_{min} \leq u \leq u_{max}$, is satisfied for all the values of p in the range of interest.

C. Baseline Controller

Table I provides the CPVs corresponding to each individual uncertain parameter for the baseline controller. The critical requirement (i.e., the one whose CPV is the closest to $\bar{p}$) corresponding to λ_m, λ_L, λ_M, λ_{CG}, and τ are g_4, g_4, g_4, g_4, and g_1 respectively. Note that λ_{CG} is the critical parameter and g_4 is most critical requirement. The PSM

TABLE I
1-DIMENSIONAL CPVS FOR d_{base}.

	$\tilde{p}^1$	$\tilde{p}^2$	$\tilde{p}^3$	$\tilde{p}^4$
$p = [\lambda_m]$	1.1847	1.1847	1.1845	1.1843
$p = [\lambda_L]$	0.5187	0.5184	0.6540	0.7036
$p = [\lambda_M]$	0.3670	0.3670	0.3897	0.4015
$p = [\lambda_{CG}]$	-0.0246	-0.0246	-0.0242	-0.0240
$p = [\tau]$	0.0310	0.0325	0.0362	0.0362

and the CPV corresponding to $p = [\lambda_{CG}, \tau]$ are equal to $\rho = 0.02564$ and $\tilde{p} = [-0.02381, 0.0095]$. As with the 1-dimensional case, the critical requirement is g_4. In the case where $p = [\lambda_m, \lambda_L, \lambda_M, \lambda_{CG}, \tau]$, the PSM, the CPV, and the critical requirement are $\rho = 0.150$, $\tilde{p} = [1.086, 0.913, 0.962, -0.0086, 8.4 \times 10^{-11}]$ and g_4 respectively.

D. Adaptive Controller

Table II shows the 1-dimensional CPVs associated with the adaptive controller. The critical requirements corresponding to λ_m, λ_L, λ_P, τ, and λ_{CG}, are now g_1, g_4, g_4, g_4, and g_1. This set of critical requirements differs from that of the baseline. As before the critical parameter is λ_{CG} and the most critical requirement is g_4. The PSM

TABLE II
1-DIMENSIONAL CPVS FOR $d_{adaptive}$.

	$\tilde{p}^1$	$\tilde{p}^2$	$\tilde{p}^3$	$\tilde{p}^4$
$p = [\lambda_m]$	0.7674	1.2347	0.7643	0.7610
$p = [\lambda_L]$	0.4606	0.4606	0.6005	0.6866
$p = [\lambda_M]$	0.2271	0.2271	0.2865	0.3629
$p = [\lambda_{CG}]$	-0.0293	-0.0293	-0.0286	-0.0267
$p = [\tau]$	0.0300	0.0316	0.0312	0.0312

[5]The reference command given is the same as that in [11].

and the CPV corresponding to $p = [\lambda_{CG}, \tau]$ are equal to $\rho = 0.02845$ and $\tilde{p} = [-0.0264, 0.0090]$. As with the 1-dimensional case, the critical requirement is g_4. In the case where $p = [\lambda_m, \lambda_L, \lambda_P, \lambda_{CG}, \tau]$, the PSM, the CPV and the critical requirement are $\rho = 0.145$, $\tilde{p} = [1.083, 0.916, 0.963, -0.009, 8.1 \times 10^{-11}]$ and g_4 respectively.

E. Comparative Analysis

The improvements in robustness resulting from augmenting the baseline controller are shown in Table III. The data in Tables I and II fully determine Table III. Note that there are directions in the uncertain parameter space where either controller outperforms the other one. This situation illustrates the tight dependence that exists between any robust control assessment method and the uncertainty model assumed. The adaptive controller attains better margins in the λ_m, λ_L, λ_M, and λ_{CG} directions. While the λ_m direction leads to the largest improvement, τ produces the only drop. Overall the augmented control architecture attains sizable improvements in all but one of the cases. Since multi-dimensional uncertainties are more realistic, cases where sizable improvements are attained, the usage of the adaptive controller is well justified. A Monte Carlo analysis of both controllers is available in [15].

TABLE III
RELATIVE PSM IMPROVEMENT.

	$\left(\frac{\rho_{adaptive}}{\rho_{baseline}} - 1\right) 100\%$
$p = [\lambda_m]$	26.2%
$p = [\lambda_L]$	5.7%
$p = [\lambda_M]$	6.5%
$p = [\tau]$	-3.2%
$p = [\lambda_{CG}]$	11.2%
$p = [\tau, \lambda_{CG}]$	7.7%
$p = [\lambda_m, \lambda_L, \lambda_P, \tau, \lambda_{CG}]$	8.2%

VI. SUMMARY

An adaptive controller for a hypersonic cruise vehicle subject to aerodynamic uncertainties, center-of-gravity movements, actuator saturation and failures, and time-delays is proposed. The control design is evaluated using a high-fidelity HSV model that considers structural flexibility and thrust-pitch coupling. An elaborate analysis of the proposed Adaptive Robust Controller for Hypersonic Vehicles (ARCH) is carried out using a stand-alone control verification methodology. This analysis indicates sizable improvements in robust performance resulting from adding an adaptive component to the baseline controller. With the exception of the time-delay margin, where a slight drop in robustness takes place, the region of safe performance was enlarged in all other one-dimensional and multi-dimensional directions of the uncertain space considered. This is particularly remarkable since the parameters and architecture of the adaptive controller were not tailored according to the system requirements.

VII. ACKNOWLEDGEMENTS

The authors would like to thank Zac Dydek, Jinho Jang and Yildiray Yildiz for several useful discussions.

REFERENCES

[1] F. R. Chavez and D. K. Schmidt, "Analytical aeropropulsive/aeroelastic hypresonic-vehicle model with dynamic analysis," *Journal of Guidance, Control, and Dynamics*, vol. 17, no. 6, 1994.
[2] M. A. Bolender and D. B. Doman, "Nonlinear longitudinal dynamical model of an air-breathing hypersonic vehicle," *Journal Spacecraft and Rockets*, vol. 44, no. 2, 2007.
[3] A. Clark, C. Wu, M. Mirmirani, S. Choi, and M. Kuipers, "An aero-propulsion integrated elastic model of a generioc airbreathing hypersonic vehicle," in *AIAA GNC Conference*, August 2006.
[4] M. A. Bolender, M. W. Oppenheimer, and D. B. Doman, "Effects of unsteady and viscous aerodynamics on the dynamics of a flexible air-breathing hypersonic vehicle," in *AIAA GAFMC*, August 2007.
[5] C. I. Marrison and R. F. Stengel, "Design of robust control systems for a hypersonic aircraft," *Journal of Guidance, Control, and Dynamics*, vol. 21, pp. 58–63, 1998.
[6] Q. Wang and R. F. Stengel, "Robust nonlinear control of a hypersonic aircraft," *Journal of Guidance, Control, and Dynamics*, vol. 23, no. 4, 2000.
[7] J. Parker, A. Serrani, S. Yurkovich, M. Bolender, and D. Doman, "Control-oriented modeling of an air-breathing hypersonic vehicle," *Journal of Guidance, Control, and Dynamics*, vol. 30, no. 3, 2007.
[8] D. . Sigthorson, P. Jankovsky, A. Serrani, S. Yurkovich, M. Bolender, and D. Doman, "Robust linear output feedback control of an airbreathing hypersonic vehicle," *Journal of Guidance, Control, and Dynamics*, vol. 31, no. 4, 2008.
[9] H. Xu, M. D. Mirmirani, and P. Ioannou, "Adaptive sliding mode control design for a hypersonic flight vehicle," *Journal of Guidance, Control, and Dynamics*, vol. 27, Sept-Oct 2004.
[10] L. Fiorentini, A. Serrani, M. A. Bolender, and D. B. Doman, "Nonlinear robust/adaptive controller design for an air-breathing hypersonic vehicle model," in *AIAA Atmospheric Flight Mechanics Conference and Exhibit*, Aug. 20-23 2007. Hilton Head, South Carolina.
[11] M. Kuipers, M. Mirmirani, P. Ioannou, and Y. Huo, "Adaptive control of an aeroelastic airbreathing hypersonic cruise vehicle," in *AIAA GNC Conference*, August 2007.
[12] T. E. Gibson and A. M. Annaswamy, "Adaptive control of hypersonic vehicles in the presence of thrust and actuator uncertainties," in *AIAA GNC Conference*, August 2008.
[13] M. Kuipers, P. Ioannou, B.Fidan, and M. Mirmirani, "Robust adaptive multiple model controller design for an airbreathing hypersonic vehicle model," in *AIAA GNC Conference*, August 2008.
[14] J. Jang, A. M. Annaswamy, and E. Lavretsky, "Adaptive flight control in the presence of multiple actuator anomalies," in *American Control Conference*, pp. 3300–3305, August 2007.
[15] T. E. Gibson, A. M. Annaswamy, and L. G. Crespo, "Adaptive pif control of hyperonsic vehicles in the presenece of modeling uncertainties," *(to be submitted) Journal of Guidance, Control, and Dynamics*, 2009.
[16] L. G. Crespo, D. P. Giesy, and S. P. Kenny, "Robust control analysis from a system requirements perspective," in *NASA TP 2009-000001*, May 2009.
[17] R. F. Stengel, *Optimal Control and Estimation*. Dover, 1994.
[18] R. F. Stengel, J. R. Broussard, and P. W. Berry, "Digital controllers for vtol aircraft," *IEEE Aerospace and Electronic Systems*, vol. 14, no. 1, pp. 54–63, 1978.
[19] K. S. Narendra and A. M. Annaswamy, *Stable Adaptive Systems*. Dover Publication, Inc., 1989.
[20] Z. Dydek, H. Jain, J. Jang, A. Annaswamy, and E. Lavretsky, "Theoretically verifiable stability margins for an adaptive controller," in *AIAA GNC Conference*, August 2006.
[21] S. P. Karason and A. M. Annaswamy, "Adaptive control in the presence of input constraints," *IEEE Transactions on Automatic Control*, vol. 39, pp. 2325–2330, May-June 1994.
[22] L. G. Crespo, D. P. Giesy, and S. P. Kenny, "Robust analysis and robust design of uncertain systems," *AIAA Journal*, vol. 46, no. 2, 2008.